Jour. Korean Inst. Mining Geol.
Vol. 26, No. 4, p. 433-444, 1993.

Mesothermal Gold-Silver Mineralization at the Bodeok Mine, Boseong Area: A Fluid Inclusion and Stable Isotope Study

Chil-Sup So*, Seong-Taek Yun**, Se-Hyun Kim***, Seung-Jun Youm*, Chul-Ho Heo* and Seon-Gyu Choi*

ABSTRACT: Electrum (32~73 atom. % Ag)-sulfide mineralization of the Bodeok mine in the Boseong area was deposited in two stages of mineralogically simple, massive quartz veins that fill the fractures along fault shear zones in Precambrian gneiss. Radiometric dating indicates that mineralization is Late Jurassic age (155.9± 2.3 Ma). Fluid inclusion data show that ore mineralization was formed from H_2O-CO_2 fluids with variable CO_2 contents (X_{CO_2}=0.0 to 0.7) and low salinities (0.0 to 7.4 wt. % eq. NaCl) at temperatures between 200° and 370℃. Evidence of fluid unmixing (CO_2 effervescence) indicates pressures up to 1 kbar. Gold-silver deposition occurred later than base-metal sulfide deposition, at temperatures near 250℃ and was probably a result of cooling and decreasing sulfur activity caused by sulfide precipitation and/or H_2S loss (through fluid unmixing).

Calculated sulfur isotope compositions of ore fluids ($\delta^{34}S_{\Sigma S}$=1.7 to 3.3‰) indicate an igneous source of sulfur in hydrothermal fluids. Measured and calculated O and H isotope compositions of ore fluids ($\delta^{18}O_{water}$=4.8 to 7.2‰, δD_{water}=−73 to −76‰) indicate that mesothermal auriferous fluids at Bodeok were likely mixtures of H_2O-rich, isotopically evolved meteoric waters and magmatic H_2O-CO_2 fluids.

INTRODUCTION

Vein-type gold-silver deposits in Korea are closely associated with major periods of Jurassic and Cretaceous granitic activity (Shimazaki et al., 1986; Shelton et al., 1988; So et al., 1989; Choi and Wee, 1992). Based on a consistent relationship among vein occurrence, gold/silver ratio of ores and electrums, vein mineralogy and paragenesis, physicochemical environments of ore formation (e.g., temperature, pressure, depth), water/rock ratio (degree of meteoric water involvement) and age of mineralization, gold-silver deposits in Korea have been classified into three to six major types (Shelton et al., 1988; So et al., 1989; Choi and Wee, 1992). Among these deposits, mesothermal to hypothermal type deposits occur characteristically in central parts of South Korea and are known to have formed during the Jurassic "Daebo" granitic activity. However, comparatively little is known about their geochemical depositional environments and origin(s) of their mesothermal to hypothermal auriferous fluids.

Geochemical studies of the Bodeok Au-Ag mine in the Boseong mineralized area were undertaken because it is the first occurrence of gold-silver mineralization in southern parts of South Korea that is contained within fissure-filling quartz veins that show characteristics of mesothermal to hypothermal-type deposits. In this paper we determine the age and nature of ore mineralization at Bodeok and document the chemistry and origin of its mesothermal gold-depositing fluids.

GENERAL GEOLOGY

The Bodeok Au-Ag mine area is located ≈20 km south of Kwangju within the Sobaegsan Massif which is composed mainly of a Precambrian gneiss complex. Geology of the mine area is very simple and is composed of Precambrian metamorphic rocks and age-unknown granites (Fig. 1).

Precambrian metamorphic rocks occupy most of the mine area, and consist of porphyroblastic gneiss, pegmatitic gneiss, and granitic gneiss. Schistosity of the metamorphic rocks strikes mainly N40°~60°E and dips 40°~60°NW. Lee (1986) suggested that metamorphic rocks of the Sobaegsan Massif formed mainly from shales and graywackes by polymetamorphism ranging from upper amphibolite to epidote-amphibolite facies with partial greenschist facies.

* Department of Geology, Korea University, Seoul 136-701, Republic of Korea
** Department of Mineral and Energy Resources Engineering, Semyung University, Jecheon 390-230, Republic of Korea
*** Department of Mineral & Mining Engineering, Sangji University, Weonju 220-702, Republic of Korea

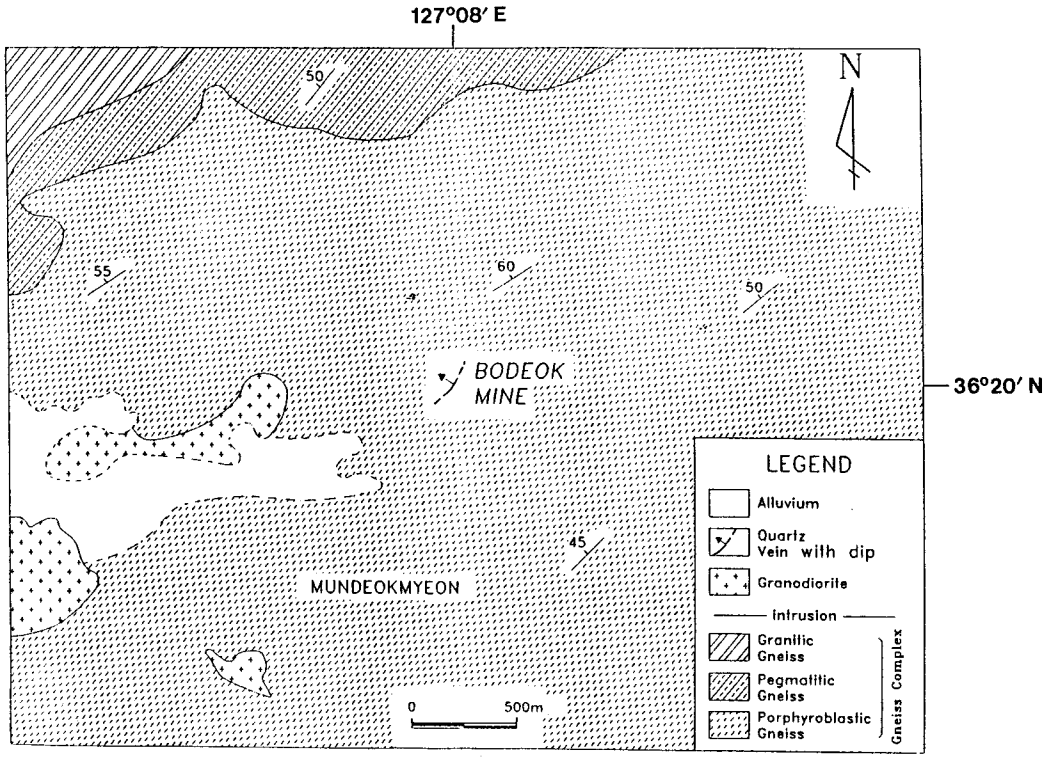

Fig. 1. Geologic map of the Bodeok Au-Ag mine area.

Age-unknown granites occur as small outcrops consisting of granodiorite, diorite, and biotite granite. Granodiorite intrudes porphyroblastic gneiss. It is composed of oligoclase, hornblende, biotite, quartz, and minor amounts of calcite and magnetite. Small pegmatite bodies and acidic dykes occur ubiquitously along faults developed in Precambrian gneiss and granodiorite.

ORE VEIN

A system of Au-Ag-bearing quartz veins of the Bodeok mine occurs as open-space fillings along fault shear zones in Precambrian gneiss (Fig. 1). The veins are often parallel to the foliation of host gneiss, and generally strike N30°~40°E with a dip of 50° NW. They run up to about 0.3 km along strike direction and vary in width from 0.1 to 1.0 m.

Electrum-base-metal sulfide mineralization at the Bodeok mine occurs in two stages of massive quartz veins which are mineralogically simple. The veins contain minor amounts (usually <5 vol. %) of ore minerals including arsenopyrite, pyrite, sphalerite, galena, electrum, and argentite. Wall-rock alteration occurs as narrow (<0.4 m wide) linear zones adjacent to vein margins, bleaching the rocks green or white. Sericitization of feldspar phenocrysts is common and fine-grained pyrites are disseminated in sericitic alteration zones.

Sericite from alteration zones yielded a K-Ar date of 155.9± 2.3 Ma (Table 1), indicating that Au-Ag mineralization at Bodeok occurred during the Late Jurassic. The massive appearance and simple mineralogy of the quartz veins at Bodeok is very similar to other gold-bearing vein deposits that formed during the Late Jurassic (Choi et al., 1988; Shelton et al., 1988; So et al., 1989).

VEIN MINERALOGY AND PARAGENESIS

Textural relationships of veins (e.g., cross-cutting and brecciation) at Bodeok indicate that they were formed in two main paragenetic stages: I and II (Fig. 2). During stage I, gray quartz with arsenopyrite, pyrite, and sphalerite was deposited. Stage II veins filled newly opened fractures and accompanied economic gold values.

Table 1. K-Ar data of alteration sericite from the Bodeok Au-Ag mine, Boseong area.

Sample no.	Description	K(%)	Radiogenic ^{40}Ar (moles/g) STP$\times 10^{-10}$	Radiogenic ^{40}Ar(%)	Date (Ma$\pm 1\sigma$)
BD-1*	Sericite from alteration zones near stage I vein	5.57	1.573	76.4	155.9$\pm$2.3

*The prepared sample contains small amounts (<5 vol. %) of kaolinite.

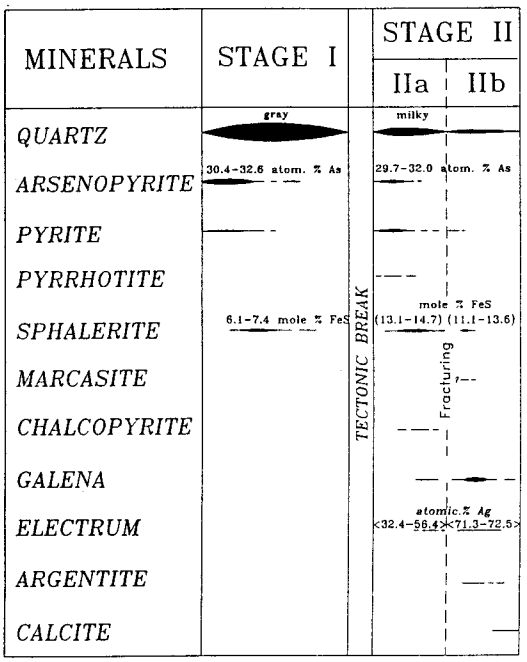

Fig. 2. Generalized paragenetic sequence of vein minerals from the Bodeok Au-Ag mine. Line widths correspond to relative abundance. [ ]; atomic % As, ( ); mole % FeS, and 〈 〉; atomic % Ag.

Stage I

Stage I mineralization is characterized by massive gray quartz with arsenopyrite. Pyrite occurs as alteration products in wall rocks and as fine, euhedral to subhedral grains within vein quartz. Pyrite aggregates at vein margins are intergrown with fine euhedral arsenopyrites (30.4~32.6 atom. % As; Table 2). Sphalerite (6.1~7.4 mole % FeS; Table 3) occurs as rims on and/or inclusions in pyrite.

Stage II

Stage II mineralization consists mainly of milky quartz with sphalerite, pyrite, galena, arsenopyrite, chalcopyrite, pyrrhotite, electrum, and argentite. Based on a fracturing event, stage II mineralization can be further divided into two substages: IIa and IIb.

During substage IIa, base-metal sulfides were mostly deposited. Pyrite occurs as subhedral to euhedral grains. Some pyrites are brecciated and cemented by galena and sphalerite. Pyrite is frequently replaced by substage IIb marcasite along grain margins and/or fractures. Arsenopyrite (29.7~32.0 atom. % As; Table 2) occurs commonly as euhedral to subhedral grains in association with pyrite. Sphalerite (13.1~14.7 mole % FeS; Table 3), the most abundant sulfide, is widespread throughout stage II veins, and occurs typically as anhedral masses. Subrounded pyrrhotite and chalcopyrite are present rarely as tiny inclusions within sphalerite. Rare, gold-rich electrum (32.4~56.4 atom % Ag, mostly less than 45%) occurs as subrounded inclusions in pyrite.

During substage IIb, sphalerite, galena, electrum, and argentite were deposited in fractures cutting quartz and sulfides of substage IIa. Stage IIb sphalerite (11.1~13.6 mole % FeS; Table 3) is associated with pyrite, galena, electrum, and argentite. Electrum (71.3 ~72.5 atom. % Ag) is associated frequently with galena and argentite. Rare calcite fills fractures in quartz.

FLUID INCLUSION STUDIES

Fluid inclusions (471 primary+pseudosecondary, 29 secondary) were examined in 42 samples of quartz and sphalerite in order to document the ranges of fluid compositions and temperatures during the mineralizing event at Bodeok. Microthermometric data were obtained on a FLUID Inc. gas-flow heating/freezing system which was calibrated with synthetic CO_2 and H_2O inclusions and various organic solvents. During freezing experiments, the sequential repeated freezing technique described by Haynes (19 85) was used for optimum precision. Salinity data are reported based on freezing point depression in the system H_2O-NaCl (Potter et al., 1978) for liquid-rich aqueous inclusions, and on clathrate melting te-

Table 2. Chemical composition of arsenopyrite from the Bodeok Au-Ag mine.

Stage	Sample no.	wt. %			Total	atomic %		
		Fe	As	S		Fe	As	S
I	BD5-1/1	34.47	44.49	20.28	99.23	33.48	32.21	34.31
	BD5-1/2	35.00	43.64	20.37	99.00	33.98	31.58	34.44
	BD3-1/1	33.72	44.60	20.57	98.88	32.80	32.34	34.86
	BD3-1/2	33.26	45.06	21.55	99.86	31.86	32.18	35.96
	BD3-1/3	34.83	44.28	21.36	100.47	33.16	31.42	35.42
	BD3-1/4	34.49	43.70	20.44	98.62	33.59	31.73	34.68
	BD3-1/5	33.87	44.81	20.16	98.85	33.08	32.62	34.30
	BD11-1/1	35.23	44.57	20.16	99.95	34.02	32.08	33.90
	BD11-1/2	35.08	44.44	20.32	99.84	33.86	31.98	34.16
	BD11-1/3	34.71	43.78	19.55	98.04	34.23	32.18	33.59
	BD3-2a/1	35.24	42.98	21.71	99.93	33.54	30.49	35.98
	BD3-2a/2	35.33	43.54	21.26	100.13	33.71	30.97	35.32
	BD3-2a/3	35.78	43.47	21.22	100.47	34.03	30.82	35.15
	BD3-2a/3″	35.78	43.41	22.05	101.23	33.58	30.37	36.04
	BD3-2a/3*	35.69	43.43	21.91	101.02	33.60	30.48	35.93
IIa	BD16-5/1	34.80	43.29	22.15	100.24	32.93	30.55	36.52
	BD16-5/1′	35.14	43.32	22.91	101.36	32.74	30.09	37.17
	BD16-5/2	34.38	42.24	23.04	99.66	32.44	29.71	37.86
	BD16-5/3	35.40	42.83	21.72	99.95	33.67	30.36	35.97
	BD16-3/1	35.01	43.57	20.10	98.67	34.16	31.69	34.15
	BD1603/2	34.45	43.63	20.00	98.08	33.84	31.95	34.21

Table 3. Chemical composition of sphalerite from the Bodeok Au-Ag mine.

Stage	Sample no.	weight percent			mole percent			Associated minerals
		Fe	Mn	Cd	FeS	MnS	CdS	
I	BD1-2	4.39	0.00	0.76	7.37	0.00	1.00	asp, py
	BD2-1	3.61	0.00	0.62	6.06	0.00	0.81	asp, py
	BD3-1	3.76	0.00	0.71	6.30	0.00	0.93	asp, py
	average	3.92	0.00	0.70	6.58	0.00	0.91	
	S.D.	0.34	0.00	0.06	0.57	0.00	0.08	
IIa	BD16-1	8.75	0.03	0.57	14.68	0.05	0.75	asp, py
	BD17	8.61	0.00	0.56	14.44	0.00	0.72	py
	BD20-2	8.79	0.03	0.32	14.75	0.05	0.42	py
	BD23	7.79	0.02	0.24	13.07	0.03	0.32	py
	BD24	8.51	0.00	0.00	14.28	0.00	0.65	py
	average	8.49	0.02	0.34	14.24	0.03	0.57	
	S.D.	0.36	0.01	0.21	0.61	0.02	0.17	
IIb	BD5-1	8.07	0.00	0.38	13.54	0.00	0.50	py, el, arg, gn
	BD5-2	8.11	0.02	0.41	13.61	0.04	0.54	py, el, arg, gn
	BD6-1	7.96	0.04	0.68	13.35	0.07	0.89	el, gn
	BD7-3	7.65	0.04	0.58	12.83	0.08	0.76	cp, el, arg, gn
	BD8	7.76	0.00	0.87	13.01	0.00	1.14	el, gn
	BD10-2	6.60	0.00	0.88	11.07	0.00	1.15	el, gn
	BD12	7.92	0.00	0.92	13.29	0.00	1.21	el, gn
	BD14	8.04	0.00	0.77	13.49	0.00	1.01	el, gn
	BD16	7.75	0.00	0.58	13.00	0.00	0.75	el, gn
	average	7.76	0.01	0.68	13.02	0.02	0.88	
	S.D	0.44	0.02	0.19	0.74	0.03	0.25	

Abbreviations: arg; argentite, asp; arsenopyrite, cp; chalcopyrite, el; electru, gn; galena, and py; pyrite.

mperatures for CO_2-bearing inclusions (Collins, 1979; Diamond, 1992).

Massive vein quartz from the Bodeok mine is inclusion-rich, probably due to repeated fracturing and healing both during and after quartz deposition. However, it was frequently difficult (if not impossible) to distinguish among primary, pseudosecondary, and secondary inclusions using normal criteria (Roedder, 1984a). Due to the difficulty of distinguishing between pseudosecondary and true primary inclusions (Shelton and Orville, 1980; Sterner and Bodnar, 19 84), a more practical distinction between primary+ pseudosecondary inclusions and obvious secondary inclusions was used.

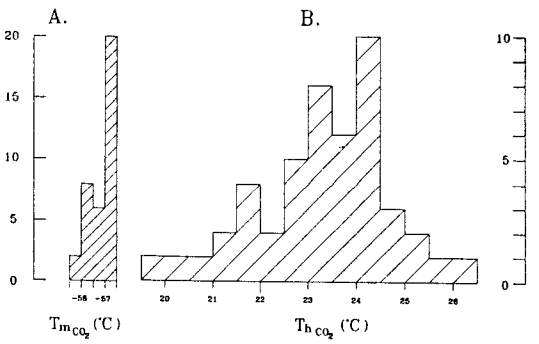

Fig. 3. Frequency diagrams of last melting temperature (A) and homogenization temperature (B) of the carbonic phase in liquid CO_2-bearing fluid inclusions in stage IIa quartz from the Bodeok Au-Ag mine.

Compositional Types of Fluid Inclusions

Two main types of fluid inclusions were recognized and classified herein based on their phase relations at 15℃ (Nash, 1972): liquid-rich aqueous inclusions (type I), and liquid CO_2-bearing inclusions (type IV).

Liquid-rich aqueous inclusions (type I) are the predominant inclusion type. They range from <5 to >30 μm in size and contain liquid and a vapor bubble comprising 20~40 volume percent at 15℃. They homogenize to the liquid phase upon heating. Type I inclusions can be further classified into two subtypes: types Ia and Ib. Type Ia inclusions are typically irregular in shape and contain a vapor bubble comprising >10% of the total inclusion volume, whereas type Ib inclusions contain a vapor bubble comprising 20~40 volume % and nucleate characteristically CO_2 hydrates during freezing. The nucleation of CO_2 hydrates in type Ib inclusions indicates that they contain minor amounts of CO_2 ($\approx$0.85 molal CO_2; Hedenquist and Henley, 1985). Type Ib inclusions are observed abundantly in stage IIb quartz and rarely in stage I quartz.

Liquid CO_2-bearing fluid inclusions (type IV) occur as obvious primary inclusions in stage IIa milky quartz. They typically contain three phases at 15℃: liquid H_2O, liquid CO_2, and vapor CO_2. The CO_2 volume proportions of type IV inclusions vary widely from 15 to 80% at 15℃. Type IV inclusions can be classified into two subtypes, based on volume proportions of CO_2 phase: CO_2-rich, and H_2O-rich. CO_2-rich type IV inclusions contain 60~80 volume % CO_2 at 15℃ and homogenize totally into a CO_2 phase upon heating, whereas H_2O-rich type IV inclusions contain 15~50 volume % CO_2 and homogenize to liquid H_2O. CO_2-only inclusions are observed rarely in stage IIa quartz, although it was difficult to assess whether they are primary or secondary in origin. The wide range of CO_2 volume % for type IV inclusions may indicate that these inclusions formed as a result of CO_2 unmixing of an initially homogeneous fluid.

Final melting temperatures of CO_2 in type IV inclusions in stage IIa quartz range from −56.5° to −58.4℃ (Fig. 3A). These temperatures indicate that the CO_2-rich phase in type IV inclusions is composed nearly of pure CO_2, although the lowest temperature (−58.4℃) may indicate a maximum CH_4 concentration of up to 5 mole % (Donelly and Katz, 1954; Burruss, 1981). Homogenization of the CO_2 phase (to liquid CO_2) in type IV inclusions occurs at temperatures between 19.8° and 26.4℃ (Fig. 3B).

Total Homogenization Temperature and Salinity

Stage I

Fluid inclusions in stage I gray quartz are mostly type Ia inclusions with some type Ib inclusions. Homogenization temperatures of primary+pseudosecondary inclusions range from 253° to 397℃ (for 34 measured type Ib inclusions, 292° to 331℃; Fig. 4). Estimated fluid salinities range from 1.2 to 4.9 wt. % eq. NaCl (for 8 measured type Ib inclusions, 1.7 to 3.2 wt. %; Fig. 5).

Stage II

Stage II minerals examined for fluid inclusion study were milky quartz and sphalerite. Due to the translucency or opacity of sphalerite, the samples for fluid inclusion study of sphalerite must be prepared as very thin, paper-like materials. Milky quartz contains all types of fluid inclusions, whereas sphalerite contains only type Ia inclusions.

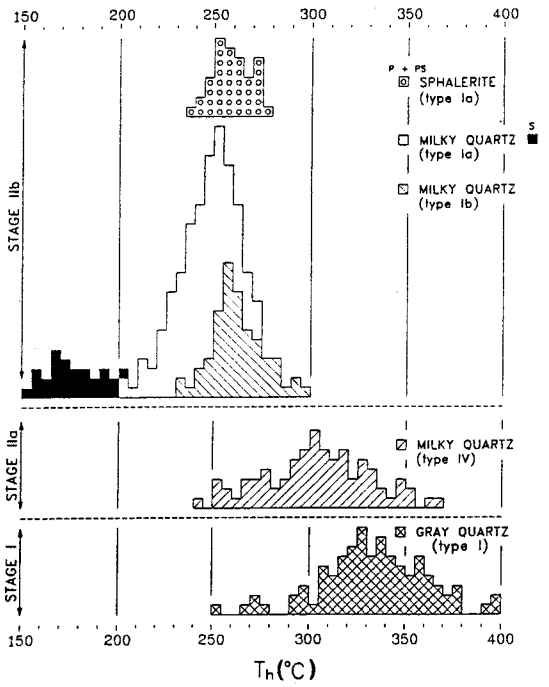

Fig. 4. Frequency diagrams of total homogenization temperatures of fluid inclusions in vein minerals from the Bodeok Au-Ag mine. P+PS; primary+pseudosecondary and S; secondary.

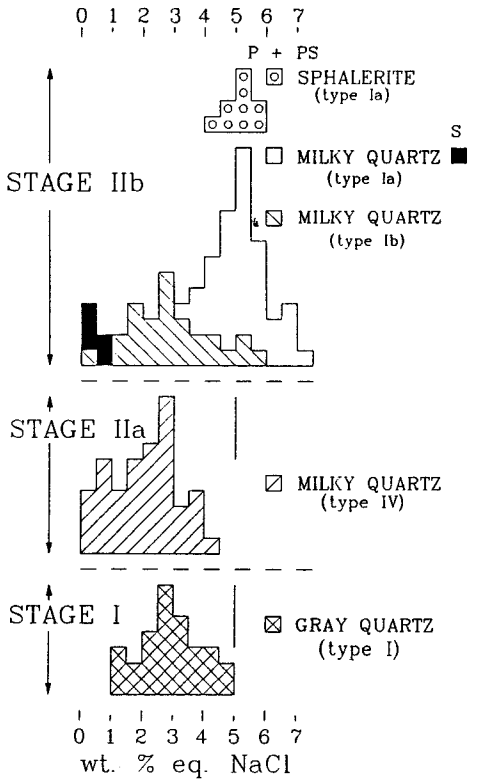

Fig. 5. Frequency diagrams of salinities of fluid inclusions in vein minerals from the Bodeok Au-Ag mine. P+PS; primary+pseudosecondary and S; secondary.

Homogenization temperatures of primary+pseudosecondary inclusions in stage II minerals range from 202° to 367℃ (for type IV inclusions in stage IIa milky quartz, 241° to 367℃; for type I inclusions in stage IIb minerals, 202° to 295℃) (Fig. 4). Within stage IIb, homogenization temperatures of primary +pseudosecondary inclusions in milky quartz range from 202° to 295℃ (type Ib inclusions, 234° to 295℃; type Ia inclusions, 202° to 273℃); those in sphalerite range from 229° to 267℃.

Salinities of primary+pseudosecondary inclusions in stage II minerals range from 0.0 to 7.4 wt. % eq. NaCl (Fig. 5). Salinities of type IV inclusions in stage IIa quartz are 0.3 to 4.4 wt. %. Within the range of fluid salinity for stage IIb milky quartz (0.0 to 7.4 wt. %), salinities of type Ib inclusions (0.0 to 5.9 wt. % eq. NaCl) are lower than those of type Ia inclusions (Fig. 5). Salinities of type Ia inclusions in sphalerite are 4.2 to 5.9 wt. % eq. NaCl.

Density and Composition of Type IV Fluid Inclusions

Bulk chemical composition and density of liquid CO_2-bearing type IV inclusions can be estimated from data on relative volumes of CO_2 and aqueous phases. Relative volumes of CO_2 and aqueous phases were estimated by measuring the enlarged inclusions with a graduated ocular (Roedder, 1984a). The density of CO_2 phase (d_{CO_2}) was determined from the homogenization temperature of CO_2 phase (Th_{CO_2}) and the mode of homogenization (Bodnar et al., 1986). The density of the aqueous phase (daq.) was calculated from the total homogenization temperature (Th_{total}) and salinity data, using the equation of Bodnar (1983). Then, the bulk density (d_{total}) of inclusion fluids was calculated using the equation: d_{total} (g/cc)= [($d_{aq.}$)×(volume fraction of aqueous phase)]+[(d_{CO_2}) ×(volume fraction of CO_2 phase)]. Bulk chemical composition of inclusion fluids were calculated using the equations described in Ramboz et al. (1985), assuming that the mole fractions of CO_2 dissolved in aqueous phase are negligible. The calculated results for some type IV inclusions are summarized in Table 4.

Calculated bulk density of the type IV inclusion

Table 4. Microthermometric data of liquid CO_2-bearing inclusions in stage IIa milky quartz from the Bodeok Au-Ag mine.

Tm_{CO_2}	Tm_{clath}	Th_{CO_2}	Th_{total}	Vol. %	density(g/cc)			wt.%			
(℃)	(℃)	(℃)	(℃)	aq.[1)]	CO_2	aq.	total	NaCl	X_{CO_2}	X_{H_2O}	X_{NaCl}
−56.7	9.9	24.1	255	85	0.72	0.79	0.73	0.2	0.06	0.94	0.00
−57.6	9.8	24.8	257	80	0.71	0.79	0.73	0.4	0.09	0.91	0.00
−56.6	9.7	25.8	260	80	0.70	0.78	0.72	0.6	0.08	0.92	0.00
−56.8	9.7	23.4	265	80	0.73	0.77	0.74	0.6	0.09	0.91	0.00
−57.1	9.9	23.9	270	65	0.73	0.76	0.74	0.2	0.17	0.83	0.00
−57.0	9.5	22.7	275	70	0.74	0.76	0.75	1.0	0.15	0.85	0.00
−57.0	9.7	26.4	275	15	0.69	0.76	0.75	0.6	0.68	0.32	0.00
−56.8	9.5	25.4	277	70	0.71	0.76	0.72	1.0	0.14	0.86	0.00
−56.9	9.6	23.0	280	80	0.74	0.75	0.74	0.8	0.09	0.91	0.00
−57.1	9.9	25.2	281	75	0.71	0.74	0.72	0.2	0.12	0.88	0.00
−57.6	9.2	22.6	281	75	0.74	0.76	0.75	1.6	0.12	0.88	0.00
−56.6	9.0	22.2	290	75	0.75	0.75	0.75	2.0	0.12	0.87	0.01
−56.7	9.3	24.8	290	80	0.71	0.74	0.72	1.4	0.09	0.91	0.00
−58.2	9.2	21.5	293	80	0.76	0.74	0.75	1.6	0.10	0.90	0.00
−58.0	9.3	21.9	295	20	0.75	0.73	0.73	1.4	0.63	0.37	0.00
−57.7	8.2	22.7	295	65	0.74	0.75	0.75	3.6	0.18	0.81	0.01
−56.6	8.7	24.7	300	80	0.72	0.73	0.72	2.6	0.09	0.90	0.01
−57.8	9.0	24.0	301	18	0.73	0.72	0.72	2.0	0.65	0.34	0.00
−56.8	8.6	21.9	307	30	0.75	0.72	0.73	2.8	0.50	0.49	0.00
−57.5	9.0	23.0	315	79	0.74	0.70	0.71	2.0	0.09	0.90	0.01
−56.7	8.5	24.5	320	20	0.72	0.70	0.70	3.0	0.63	0.36	0.00
−56.6	8.7	23.5	328	30	0.73	0.70	0.70	2.6	0.51	0.48	0.00
−57.5	8.9	23.2	329	70	0.74	0.67	0.72	2.2	0.16	0.83	0.01
−56.6	8.6	22.3	330	57	0.75	0.68	0.72	2.8	0.26	0.74	0.01
−56.7	8.5	22.3	335	60	0.75	0.67	0.72	3.0	0.24	0.76	0.01
−56.5	8.4	19.8	340	65	0.78	0.66	0.74	3.2	0.21	0.78	0.01

[1)] Visual estimate at 15℃.

Abbreviations: aq; aqueous phase, clath; CO_2 clathrate, Th; homogenization temperature, and Tm; melting temperature.

fluids ranges from 0.70 to 0.75 g/cc (Table 4). Calculated molar fractions of CO_2 (X_{CO_2}) are (Table 4): for H_2O-rich inclusions, 0.06 to 0.26 (mostly less than 0.15); and for CO_2-rich inclusions, 0.50 to 0.68.

Variation in Temperature and Composition of Hydrothermal Fluids

Wide range of homogenization temperature (≈ 200° to 400℃; Fig. 4) of fluid inclusions in vein minerals from the Bodeok mine probably reflects several hydrothermal episodes rather than one specific event. The upper ends of homogenization temperatures are 400℃ for stage I and 370℃ for stage II mineralization. Combined with the abundance of liquid CO_2-bearing fluid inclusions, such high temperatures for hydrothermal fluids indicate that the vein mineralization at Bodeok belongs to mesothermal-hypothermal type deposits. However, the relatively lower homogenization temperatures (≈ 225° to 270℃) for fluid inclusions in sphalerite which is closely associated with gold and silver minerals indicate that main Au-Ag deposition occurred at temperatures near 250℃. It is also noteworthy that the ranges and peaks of homogenization temperatures decrease gradually with time (Fig. 4), likely due to progressive cooling of the hydrothermal fluids.

As described previously, hydrothermal fluids observed in stage II minerals are composed of two types: (1) dominantly aqueous fluids of moderate salinity (type I), occasionally containing minor amounts of CO_2 (type Ib), and (2) mixed CO_2-H_2O fluids of low salinity (type IV). CO_2 contents of the type IV fluid inclusions are highly variable within individual samples. The more CO_2-rich type IV inclusions homogenized at nearly the same temperatures as more H_2O-rich type IV inclusions. These observations indicate that the type IV fluid inclusions represent the trapping of immiscible H_2O-CO_2 fluids which evolved through CO_2 effervescence.

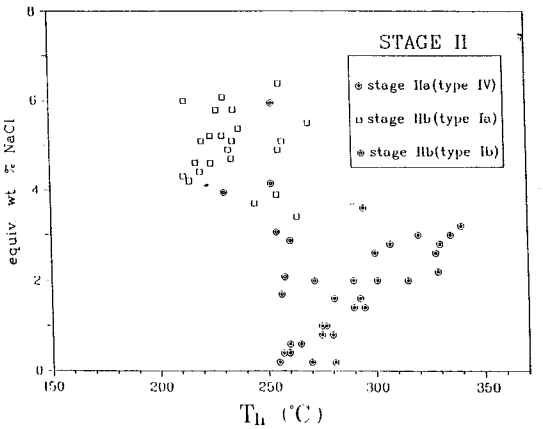

Fig. 6. Salinity versus homogenization temperature diagram for primary and pseudosecondary fluid inclusions in stage II quartz from the Bodeok Au-Ag mine.

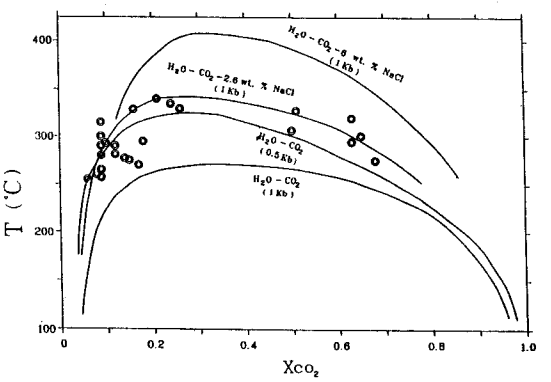

Fig. 7. Mole fraction of CO_2 (X_{CO_2})-temperature diagram showing the two-phase immiscibility curves for H_2O-CO_2 (−NaCl) fluids at different pressures (after Tödheide and Franck, 1963; Hendel and Hollister, 1981; Bowers and Helgeson, 1983b). Data are for liquid CO_2-bearing fluid inclusions in stage IIa quartz from the Bodeok Au-Ag mine.

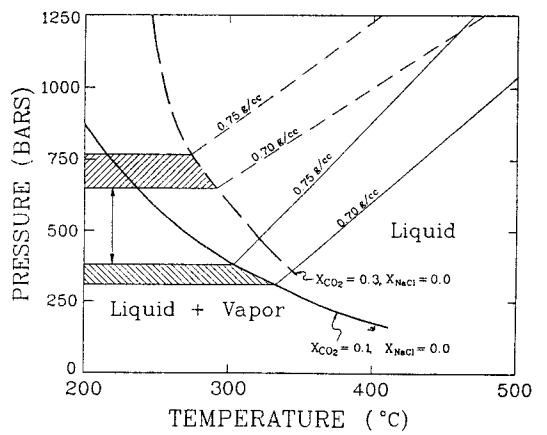

Fig. 8. Temperature-pressure diagram showing the two-phase solvus curves and isochores for H_2O-CO_2 fluids (after Bowers and Helgeson, 1983a). Hatched fields represent the estimated pressure conditions for entrapment of liquid CO_2-bearing fluid inclusions in stage IIa quartz from the Bodeok Au-Ag mine.

The relationship between homogenization temperature and salinity for gold-silver-depositing stage II fluids is shown in Fig. 6. Liquid CO_2-bearing type IV inclusions in stage IIa quartz show a decreasing salinity (from ≈4 to 0 wt. % eq. NaCl) with decreasing temperature from 340° to 250°C. This trend is explained by the boiling (CO_2 effervescence) of CO_2-rich ("high gas") fluids, although this trend also may result from simple cooling (Hedenquist and Henley, 1985). The CO_2-poor fluids which remained after extensive escape of CO_2 gas were probably trapped at temperatures between 270°C and 230°C (Fig. 4) as CO_2 clathrate-forming type Ib inclusions in stage IIb quartz. Type Ib inclusions tend to show an increasing salinity (from <2 to 6 wt. % eq. NaCl) with decreasing temperature, likely indicating the extensive continued boiling of CO_2-poor fluids. Such continued boiling of hydrothermal fluids is thought to be the result of pressure decrease during the ascent of hydrothermal fluids. Following the complete loss of CO_2 from stage II fluids, the residual fluids were trapped as CO_2-absent type Ia fluid inclusions (T_h°C=200°~275°C; Fig. 4) in quartz and sphalerite. The close association of gold-silver minerals with stage IIb sphalerite indicates that the fluids present during Au-Ag deposition at Bodeok were predominantly H_2O-rich.

Fluid boiling accompanying CO_2 effervescence in hydrothermal systems may result in abrupt chemical changes in the liquid phase (e.g., fo_2, $_2H_2S$). These changes may favor deposition of precious metals through destabilization of metal complexes (Seward, 1973, 1984; Drummond and Ohmoto, 1985; Cole and Drummond, 1986). Gold precipitation mechanisms involving gold bisulfide complex include a decrease in temperature at constant pH, oxidation of the complex, pH decrease, and decrease of sulfur activity by sulfide precipitation and/or H_2S loss accompanying boiling. Several of these possibilities are illustrated by the reaction: $Au(HS)_2^- + 1/2H_{2(g)} + H^+ = Au^0 + 2H_2S_{(aq)}$. Given the frequent association of galena, sphalerite, and chalcopyrite with gold in the Bodeok mine, the role of sulfide precipitation accompanying boiling is critical. We suggest that decrease of sulfur activity

Table 5. Sulfur isotope data for stage II sulfide minerals from the Bodeok Au-Ag mine.

Substage	Sample No.	Mineral	$\delta^{34}S$ (‰)	$\Delta^{34}S$ (‰)	T(℃)[2]	$\delta^{34}S_{H_2S}$ (‰)[3]
IIa	BD-16-1	arsenopyrite	3.6		325	3.3
	BD-17-1	pyrite	3.4		310	2.2
	BD-20-3	sphalerite	3.2		330	2.9
	BD-22-1	sphalerite	2.6		280	2.3
	BD-25-1	pyrite	3.2		340	2.1
	BD-25-2	chalcopyrite	2.0		340	2.1
IIb	BD-5-3	sphalerite	2.3		250	1.9
	BB-7-3	galena	0.0		260	2.2
	BD-12-1	galena	0.3		250	2.6
	BD-33-1	sphalerite	2.1	sp-gn	244	1.7
	BD-33-2	galena	−0.5	2.6 (254± 30)[1]	244	1.7

[1] Number in parenthesis is sulfur isotope temperature calculated using the equation in Ohmoto and Rye (1979).
[2] Based on fluid inclusion and/or sulfur isotope temperatures and paragenetic constraints.
[3] Calculated sulfur isotope compsitions of H_2S in ore fluids, using the isotope fractionation equation in Ohmoto and Rye (1979).

Table 6. Oxygen and hydrogen isotope data for stage II quartz from the Bodeok Au-Ag mine.

Sample no.	Mineral	$\delta^{18}O$(‰)	T(℃)	$\delta^{18}O_{water}$(‰)[2]	δD(‰)
BD-8-1	quartz	11.5	280 to 320 (305)	3.9 to 5.3 (4.8)	−75
BD-10-3	quartz	12.3	272 to 320 (300)	4.4 to 6.1 (5.4)	−76
BD-16	quartz	13.2	293 to 348 (325)	6.1 to 7.8 (7.2)	−73
BD-22-2	quartz	12.6	269 to 327 (290)	4.1 to 6.6 (5.4)	−75
BD-24-1	quartz	13.1	258 to 338 (295)	4.6 to 7.5 (6.1)	−75

[1] Ranges of fluid inclusion homogenization temperatures. Numbers in parentheses are average values.
[2] Calculated water compositions based on oxygen isotope fractionation equation of Matsuhisa et al. (1979).

accompanying boiling, through sulfide deposition and/or H_2S loss, is likely the most important mechanism for gold deposition in the mesothermal-type vein deposits at Bodeok.

Pressure Consideration

Data of P-T-X relations on the system H_2O-CO_2-NaCl can be used to estimate the evolution of CO_2-rich hydrothermal fluids and the pressure conditions of fluid entrapment. Fig. 7 shows the relations between the estimated compositions of type IV inclusion fluids (Table 4) and the two-phase (solvus) curves for the system H_2O-CO_2(−NaCl). The two-phase curve of the H_2O-CO_2 system moves toward lower temperatures by increasing pressure (Tödheide and Franck, 1963; Takenouchi and Kennedy, 1965). Addition of NaCl to the H_2O-CO_2 fluids raises the two-phase curve (Danneil et al., 1967; Gehrig, 1980; Hendel and Hollister, 1981; Bowers and Helgeson, 1983a). The data from Bodeok fall mostly between two-phase curves of an H_2O-CO_2-6.0 wt. % NaCl fluid at 1 kbar and an H_2O-CO_2 fluid at 1 kbar. The data tend to run subparallel with the two-phase curve of an H_2O-CO_2-2.6 wt. % NaCl fluid at 1 kbar. There is a compositional gap at the X_{CO_2} range of 0.25 to 0.5 (Fig. 7).

These observations may indicate that the fluids in liquid CO_2-bearing type IV inclusions were entrapped at or near the two-phase boundary (boiling conditions). Fluid inclusions with the highest homogenization temperatures (near 340℃) have X_{CO_2} values of 0.2 to 0.25 and plot on or near the two-phase curve of an H_2O-CO_2-2.6 wt. % NaCl fluid at 1 kbar. These fluid inclusions are thought to represent the initial homogeneous fluid and, therefore, indicate fluid pressures at the time of entrapment of about 1 kbar.

Fig. 8 shows the two-phase curves for the H_2O-CO_2 system on a temperature versus pressure diagram, with X_{CO_2} of 0.1 and 0.3 (Bowers and Helgeson, 1983 a). The distribution of our data on a temperature versus X_{CO_2} diagram (Fig. 7) indicated that the parent homogeneous fluids probably had X_{CO_2} values less than 0.3. Combined with the calculated bulk densities (d_{total}=0.70~0.75 g/cc for type IV fluid inclusions), the evidence of fluid boiling (CO_2 effervescence) indicates a range of fluid pressures of about 300

to 750 bars (Fig. 8). The two-phase curves and the isochores (Fig. 8) also show that trapping temperatures must have been in the range of 270° to 330℃, which is in agreement with homogenization temperatures (240°~370℃, Fig. 4) of fluid inclusions. However, this range of fluid pressures must be considered as a minimum estimate because the addition of NaCl to the system moves the two-phase curves toward much higher pressures (Bowers and Helgeson, 1983 a). We suggest that fluid pressures during the mineralizing event at Bodeok approached 1 kbar. This pressure corresponds to minimum depths of 3.5 to 10.0 km, assuming lithostatic and hydrostatic pressure conditions, respectively.

STABLE ISOTOPE STUDIES

Sulfur isotope compositions of sulfide minerals, oxygen isotope compositions of quartz, and hydrogen isotope compositions of inclusion waters extracted from quartz were measured in order to interpret the source(s) and evolution of ore constituents in the hydrothermal fluids at Bodeok. Standard techniques of extraction and analysis was used, as described by Grinenko (1962) and Hall and Friedman (1963). Data are reported in standard δ notation relative to the CDT standard for S, and Vienna SMOW for O and H. The standard error of each analysis is approximately 0.1 per mil for S and O, and 2 per mil for H.

Sulfur Isotope Study

Sulfur isotope analyses were performed on 11 monomineralic samples from stage II veins (Table 5). The minerals measured have $\delta^{34}S$ values of -0.5 to 3.6 per mil. One sphalerite-galena pair from stage IIb vein has a $\Delta^{34}S$ value of 2.6 per mil, yielding an equilibrium isotope temperature of 254°± 30℃ (Ohmoto and Rye, 1979), in agreement with fluid inclusion temperatures in associated quartz.

Assuming appropriate depositional temperatures for each sample (based on fluid inclusion and paragenetic constraints), the $\delta^{34}S$ values of H_2S in hydrothermal fluids are calculated to be 1.7 to 3.3 per mil (Table 5). The narrow range of $\delta^{34}S$ values of sulfide minerals and the presence of pyrrhotite in veins indicate that sulfur was present dominantly as reduced sulfur (H_2S). Therefore, the calculated range of $\delta^{34}S$ values of H_2S may be taken as the sulfur isotope composition of entire fluid ($\delta^{34}S_{\Sigma S}$). The $\delta^{34}S_{\Sigma S}$ values of 1.7 to 3.3 per mil indicate a likely igneous source of sulfur in the Bodeok hydrothermal fluids (Ohmoto and Rye, 1979).

Oxygen and Hydrogen Isotope Study

Five samples of stage II vein quartz were prepared and measured for oxygen and hydrogen isotope compositions (Table 6). The $\delta^{18}O$ values are 11.5 to 13.2 per mil. Using the quartz-water oxygen isotope fractionation equation of Matsuhisa et al. (1979), coupled with fluid inclusion temperatures, the calculated $\delta^{18}O$ values of waters in equilibrium with quartz are 3.9~5.3 (average 4.8) to 6.1~7.8 (average 7.2) per mil. Inclusion waters extracted from the quartz samples by crushing have uniform δD values of -73 to -76 per mil (Table 6).

The measured and calculated oxygen and hydrogen isotope compositions of the hydrothermal fluids at Bodeok can be used to assess the importance of meteoric, magmatic, and metamorphic waters in the gold-mineralized mesothermal systems. Although the $\delta^{18}O_{water}$ values for the Bodeok fluids (3.9~7.8‰) are slightly lower than the range of magmatic water isotopic compositions ($\delta^{18}O$=5.5 to 10‰, δD=-40 to -80‰; Taylor, 1974), the overlap of the δD data may reflect the input of a primary magmatic water component to the ore fluids. This could occur through mixing between an isotopically evolved meteoric water and a magmatic H_2O-CO_2 fluid, as proposed for the Mink Lake Archean gold deposits by Burrows and Spooner (1987). The common occurrence of liquid CO_2-bearing fluid inclusions in Jurassic granites of Korea was recognized by Watanabe (1981). The CO_2-rich character of the inclusion fluids from the Jurassic Bodeok mine may indicate a significant contribution of fluids from Jurassic granitic melts. Our data are not compatible with ore formation from metamorphic fluids ($\delta^{18}O$=4 to 25‰, δD=-20 to -65‰).

ACKNOWLEDGEMENTS

This research was supported as a research project among Special Research and Development Programs sponsored by the Republic of Korea's Ministry of Science and Technology. The authors acknowledge Prof. Kevin L. Shelton and Dr. Choi, S.H. for their fruitful comments and constructive improvements of the manuscript. The authors are indebted to Lee, J. H., Kweon, S.H., Choi, K.J., and Lee, D.H. for their assistance with field survey and sample preparations.

REFERENCES

Bodnar, R.J. (1983) A method of calculating fluid inclusion volumes based on vapor bubble diameters and P-V-T-X properties of inclusion fluids. Econ. Geol., v. 78, p. 535-542.

Bodnar, R.J., Reynolds, T.J. and Kuehn, C.A. (1986) Fluid-inclusion systematics in epithermal systems. In Berger, B.R. and Bethke, P.M. eds., Geology and geochemistry of epithermal systems. Reviews in Economic Geology, v. 2, p. 73-97.

Bowers, T.S. and Helgeson, H.C. (1983a) Calculation of the thermodynamic and geochemical consequences of nonideal mixing in the system H_2O-CO_2-NaCl on phase relations in geologic systems: Equation of state for H_2O-CO_2-NaCl fluids at high pressures and temperatures. Geochim. et Cosmochim. Acta, v. 47, p. 1247-1275.

Bowers, T.S. and Helgeson, H.C. (1983b) Calculation of the thermodynamic and geochemical consequences of nonideal mixing in the system H_2O-CO_2-NaCl on phase relations in geologic systems: Metamorphic equilibria at high pressures and temperatures. Am. Mineral., v. 68, p. 1059-1075.

Burrows, D.R. and Spooner, E.T.C. (1987) Generation of a magmatic H_2O-CO_2 fluid enriched in Mo, Au, and W within an Archean sodic granodioritic stock, Mink Lake, northwestern Ontario. Econ. Geol., v. 82, p. 1931-1957.

Burruss, R.C. (1981) Analysis of fluid inclusions: Phase equilibria at constant volume. Am. Jour. Sci., v. 281, p. 1104-1126.

Choi, S.G. and Wee, S.M. (1992) The genetic characteristics of gold and/or silver vein deposits related to chemical composition of electrum in central Korea. Jour. Geol. Soc. Korea, v. 28, p. 196-217 (in Korean).

Choi, S.G., Chi, S.J. and Park, S.W. (1988) Gold-silver mineralization of the Au-Ag deposits at Youngdong district, Chungcheongbuk-Do. Jour. Korean Inst. Mining Geol., v. 21, p. 367-380 (in Korean).

Cole, D.R. and Drummond, S.E. (1986) The effect of transport and boiling on Ag/Au ratios in hydrothermal solutions: A preliminary assessment and possible implications for the formation of epithermal precious-metal ore deposits. Jour. Geochem. Explor., v. 25, p. 45-79.

Collins, P.L.F. (1979) Gas hydrates in CO_2-bearing fluid inclusions and the use of freezing data for estimation of salinity. Econ. Geol., v. 74, p. 1435-1444.

Danneil, A., Tödheide, K. and Franck, E.U. (1967) Verdampfungsgleichgewichte und kritische Kurven in den Systemen Äthan/Wasser und n-Butan/Wasser bei hohen Drücken. Chem. Ing. Tech., v. 39, p. 816-822 (in German).

Diamond, L.W. (1992) Stability of CO_2 clathrate hydrate+CO_2 liquid+CO_2 vapor+aqueous KCl-NaCl solutions: Experimental determination and application to salinity estimates of fluid inclusions. Geochim. et Cosmochim. Acta, v. 56, p. 273-280.

Donelly, H.G. and Katz, D.L. (1954) Phase equilibria in the carbon dioxide-methane system. Ind. Eng. Chem., v. 46, p. 511-517.

Drummond, S.E. and Ohmoto, H. (1985) Chemical evolution and mineral deposition in boiling hydrothermal systems. Econ. Geol., v. 80, p. 126-147.

Gehrig, M. (1980) Phasengleichgewichte und PVT-Daten ternärer Mischungen aus Wasser, Kohlendioxid und Natriumchlorid bis 3 kbar und 550℃. Univ. Karlsruhe, Ph.D. thesis, Hochschul Verlag, Freiburg (in German).

Grinenko, V.A. (1962) Preparation of sulfur dioxide for isotopic analysis. Zeitschr. Neorgan. Khimii., v. 7, p. 2478-2483.

Hall, W.E. and Friedman, I. (1963) Composition of fluid inclusions, Cave-in-Rock fluorite district, Illinois and Upper Mississippi Valley zinc-lead district. Econ. Geol., v. 58, p. 886-911.

Haynes, F.M. (1985) Determination of fluid inclusion compositions by sequential freezing. Econ. Geol., v. 80, p. 1436-1439.

Hedenquist, J.W. and Henley, R.W. (1985) The importance of CO_2 on freezing point measurements of fluid inclusions: Evidence from active geothermal systems and implications for epithermal ore deposition. Econ. Geol., v. 80, p. 1379-1406.

Hendel, E.M. and Hollister, L.S. (1981) An empirical solvus for CO_2-H_2O-2.6 wt. % salt. Geochim. et Cosmochim. Acta, v. 45, p. 225-228.

Lee, S.W. (1986) Metamorphism of the gneiss complex in the southwestern region of the Sobaegsan Massif. In Memoirs in celebration of the sixtieth birthday of Professor Sang Man Lee, Seoul Natl. Univ., Seoul, p. 133-153 (in Korean).

Matsuhisa, Y., Goldsmith, R. and Clayton, R.N. (1979) Oxygen isotope fractionation in the system quartz-albite-anorthite-water. Geochim. et Cosmochim. Acta, v. 43, p. 1131-1140.

Nash, J.T. (1972) Fluid inclusion studies of some gold deposits in Nevada. U.S. Geol. Survey Prof. Paper 800-C, p. 15-19.

Ohmoto, H. and Rye, R.O. (1979) Isotopes of sulfur and carbon. In Barnes, H.L. ed., Geochemistry of hydrothermal ore deposits. New York, Wiley Intersci., p. 509-567.

Potter, R.W., III, Clynne, M.A. and Brown, K.L. (1978) Freezing point depression of aqueous sodium chloride solutions. Econ. Geol., v. 73, p. 284-285.

Ramboz, C., Schnapper, D. and Dubessy, J. (1985) The P-V-T-X-fo_2 evolution of H_2O-CO_2-CH_4-bearing fluid in a wolframite vein: Reconstruction from fluid inclusion studies. Geochim. et Cosmochim. Acta, v. 49, p. 205-219.

Roedder, E. (1984) Fluid inclusions. Rev. Mineralogy, v. 12, 644p.

Seward, T.M. (1973) Thio complexes of gold and the transport of gold in hydrothermal ore solutions. Geochim. et Cosmochim. Acta, v. 37, p. 379-399.

Seward, T.M. (1984) The transport and deposition of gold in hydrothermal systems. In Foster, R.P. ed., Gold '82. Rotterdam, A.A. Balkema Pub., p. 165-181.

Shelton, K.L. and Orville, P.M. (1980) Formation of synthetic fluid inclusions in natural quartz. Am. Mineral.,

v. 65, p. 1233-1236.
Shelton, K. L., So, C. S. and Chang, J. S. (1988) Gold-rich mesothermal vein deposits of the Republic of Korea: Geochemical studies of the Jungwon gold area. Econ. Geol., v. 83, p. 1221-1237.
Shimazaki, H., Lee, M. S., Tsusue, A. and Kaneda, H. (1986) Three epochs of gold mineralization in South Korea. Mining Geology, v. 36, p. 265-272.
So, C. S., Yun, S. T. and Chi, S. J. (1989) Geochemical studies of hydrothermal gold-silver deposits, Republic of Korea: Yangdong mining district. Jour. Geol. Soc. Korea, v. 25, p. 16-29.
Sterner, S. M. and Bodnar, R. J. (1984) Synthetic fluid inclusions in natural quartz. I. Compositional types synthesized and applications to experimental geochemistry. Geochim. et Cosmochim. Acta, v. 48, p. 2659-2668.
Takenouchi, S. and Kennedy, G. C. (1965) The solubility of carbon dioxide in NaCl solutions at high temperatures and pressures. Am. Jour. Sci., v. 263, p. 445-454.
Taylor, H. P., Jr. (1974) The application of oxygen and hydrogen isotope studies to problems of hydrothermal alteration and ore deposition. Econ. Geol., v. 69, p. 843-883.
Tödheide, K. and Franck, E.U. (1963) Das zweiphasengebiet und die kritische kurve in system kohlendioxid-wasser bis zu drucken von 3500 bar. Z. Phys. Chem. N. F., v. 37, p. 387-401 (in German).
Watanabe, M. (1981) Reconnaisance study on the fluid inclusions in some Jurassic and Cretaceous granitic rocks in the Republic of Korea. In Tsusue, A. ed., Petrographic provinces of granitoids and associated metallic ore deposits in South Korean peninsula. Kumamoto, Japan, Kumamoto Univ., Overseas Field Research Rept., p. 109-124.

Manuscript received 20 June 1993

全南 寶城地域 寶德鑛山의 深部 中溫型 金-銀 鑛化作用: 流體包有物 및 安定同位元素 硏究

蘇七燮 · 尹聖澤 · 金世鉉 · 廉承竣 · 許哲豪 · 崔善奎

요 약: 全南 寶城지역 寶德 광산의 에렉트럼 (銀함량=32~73 atom. %)-황화광물 鑛化作用은 선캠브리아紀 片麻岩내의 斷層 열극을 충진한 石英脈으로 산출된다. 석영맥은 광물조성이 단순한 塊狀이며, 構造적으로 2회에 걸쳐 형성되었다. 熱水變質帶 絹雲母에 대한 K-Ar 연령은 155.9± 2.3 Ma로서 鑛化作用이 후기 쥬라紀에 일어났음을 지시한다. 流體包有物 연구에 의하면, 鑛化作用은 다양한 CO_2 함량 (X_{CO_2}=0.0~0.7)과 低鹽度 (0.0~7.4 wt. % NaCl 相當濃度)를 갖는 H_2O-CO_2系 流體로부터 200°~370℃ 의 溫度범위에서 진행되었다. 鑛化流體의 不混和 (CO_2 沸騰) 증거는 鑛化作用시의 壓力이 약 1 kbar에 이르렀음을 지시한다. 金-銀 沈澱은 base-metal系 黃化鑛物 보다는 후기, 약 250℃ 근처에서 진행되었고, 流體 不混和에 따라 黃化鑛物 沈澱 및 H_2S 일탈이 야기되면서 주로 冷却 및 硫黃分壓의 감소에 기인하였다.

鑛化流體의 硫黃同位元素 조성 ($\delta^{34}S_{\Sigma S}$=1.7~3.3‰)은 硫黃의 火成기원을 나타낸다. 한편, 鑛化流體의 酸素-水素 同位元素 조성 ($\delta^{18}O_{water}$=4.8~7.2‰; δD_{water}=−73~−76‰)은, 寶德광산의 深部 中溫型 含金 鑛化流體는 同位元素的으로 진화된 H_2O-rich 循環天水와 深部 magma 기원의 H_2O-CO_2 流體와의 混合物로부터 기원했음을 지시한다.